Geotechnical Research
Volume 1 Issue 4

Simplified finite-element modelling for tunnelling-induced settlements
Likitlersuang, Surarak, Suwansawat *et al*.

Geotechnical Research, 2014, **1**(4), 133–152
http://dx.doi.org/10.1680/gr.14.00016
Paper 14.00016
Received 03/09/2014; accepted 06/11/2014
Published online 06/12/2014
Keywords: monitoring/numerical modelling/tunnels

ice
Institution of Civil Engineers
publishing

Simplified finite-element modelling for tunnelling-induced settlements

1 **Suched Likitlersuang**
Professor, Department of Civil Engineering, Faculty of Engineering, Chulalongkorn University, Bangkok, Thailand

2 **Chanaton Surarak**
Lieutenant Colonel, 111th Engineer Battalion, Royal Thai Army, Thailand

3 **Suchatvee Suwansawat**
Professor, Civil Engineering Department, Faculty of Engineering, King Mongkut's Institute of Technology Ladkrabang, Bangkok, Thailand

4 **Dariusz Wanatowski**
Associate Professor, Faculty of Science and Engineering, University of Nottingham Ningbo, China

5 **Erwin Oh**
Senior Lecturer, School of Engineering, Griffith University, Gold Coast Campus, Queensland, Australia

6 **Arumugam Balasubramaniam**
Professor, School of Engineering, Griffith University, Gold Coast Campus, Queensland, Australia




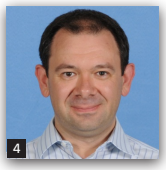

Tunnelling-induced ground surface settlement prediction still adopts empirical and analytical approaches; thus a step further in using a practical numerical analysis is now a challenging task. Because the deformation during tunnelling is a three-dimensional problem, several features were incorporated in two-dimensional analyses to capture aspects that are important in governing behaviour in the missing third dimension. This paper aims to present simplified methods for ground settlement computation of tunnelling works using the PLAXIS finite-element programme. Three simplified methods – contraction ratio, stress reduction and modified grout pressure – were considered in this study. Practical application requires correlations among these three methods. Such correlations among the three methods are proposed in this study and can be used in geotechnical practice. The results were based on a series of finite-element analyses of the Blue Line Bangkok Mass Rapid Transit tunnels. The geotechnical parameters were selected based on soil investigation reports carried out for construction purposes. The soil constitutive model adopted herein was the hardening soil model on soft and stiff clays. All the finite-element simulations were compared with the measured field deformations. Therefore, the analysis results can be considered as a Class-C prediction (back-analysis).

Notation

c'	cohesion
D	tunnel diameter
E_{50}^{ref}	reference secant modulus from drained triaxial test
E_{oed}^{ref}	reference tangent modulus for oedometer primary loading
E_{ur}^{ref}	reference unloading/reloading modulus
G_p	physical gap
H	distance from the ground surface to tunnel crown
h	distance from the tunnel crown to the bottom boundary
i	distance of the inflection point
K_0^{nc}	coefficient of earth pressure at rest (NC state)
m	exponential power for modulus
p_F	face pressure
p_o	initial support pressure
p^{ref}	reference pressure (100 kN/m^2)
R_f	failure ratio
w	width of the model
β	unloading factor
γ_g	unit weight of grout
γ_s	unit weight of the slurry
δ_{max}	maximum settlement at tunnel centre line
ν_{ur}	unloading/reloading Poisson's ratio
σ_v	total vertical stress
ϕ'	internal friction angle
ψ	dilatancy angle

Introduction

Tunnelling and underground construction in soft ground are usually associated with substantial difficulties. Because the soft soils are sensitive to deformations and possess small shear strength, they may lead to structural damage during the construction as well as

throughout the life of the structures. It is well known that Bangkok metropolitan area is located on a thick soft to very soft clay layer on the top deposit. One of the most recent important infrastructure improvement projects in Bangkok is the construction of the Mass Rapid Transit (MRT) underground railway. This project involves significant geotechnical works, especially deep foundations and excavations.

The finite-element method (FEM) has become an increasingly popular and powerful analytical tool for modelling construction works. Several in-house finite-element codes developed by research groups are, however, unfriendly to users and therefore seldom used in practice. As a result, commercial finite-element software specifically written for solving geotechnical problems has become very popular and useful among practising engineers. Various finite-element modelling methods from simple two-dimensional (2D) linear elastic to complex three-dimensional (3D) non-linear elastic-plastic analyses have been developed to explain the behaviour of tunnels in soft grounds. However, there is still a problem with prediction of ground movements induced by tunnelling with the use of FEM. The results of numerical analysis may be influenced by many factors such as simplified geometry and boundary conditions, mesh generation, initial input of ground conditions and constitutive relationships chosen to model the behaviour of soils.

This paper aims to present simplified finite-element analyses of tunnelling-induced surface settlement based on the Blue Line Bangkok MRT project. This is one of a series of numerical studies related to Bangkok clay behaviour (Likitlersuang *et al.*, 2013a, 2013b, 2013c; Surarak *et al.*, 2012). The stiffness and strength parameters of Bangkok clay used for the hardening soil model (HSM) were earlier described by Surarak *et al.* (2012). Likitlersuang *et al.* (2013c) also described the small strain stiffness and the stiffness degradation curve. The finite-element analysis of the deep excavation of the Bangkok MRT station was also studied and reported in Likitlersuang *et al.* (2013a). The geotechnical parameters from pressuremeter tests for Bangkok MRT project were presented in Likitlersuang *et al.* (2013b). This paper therefore aims to continue the finite-element analysis of tunnelling in the soft Bangkok clay based on the previous studies of the authors. The finite-element software PLAXIS was selected as a numerical tool and the Bangkok MRT tunnel construction was chosen as a case study. This study focuses on the use of three simplified methods – the contraction ratio method, the stress reduction method and the modified grout pressure method – to back-analyse ground

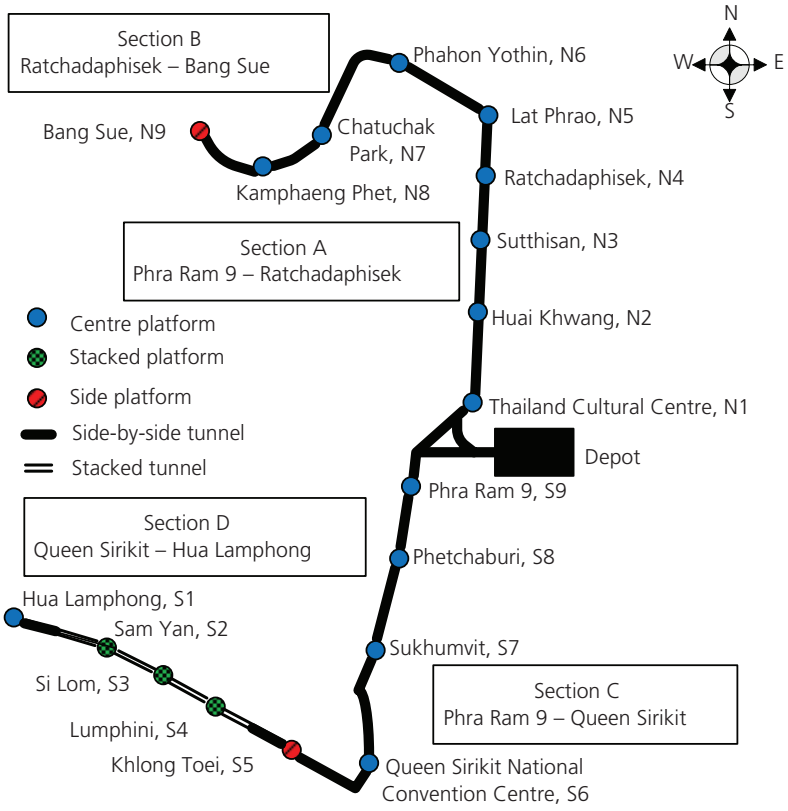

Figure 1. Bangkok MRT Blue Line route

settlement due to tunneling works. All the back-analysis results are compared with the field monitoring data in order to assess the validity of the chosen methods.

Bangkok MRT project

The first phase of the Bangkok MRT Underground Railway, named the Chaloem Ratchamongkhon (or Blue Line) between Hua Lamphong and Bang Sue, was completed in 2004. It comprises approximately 20 km of tunnels, constructed using tunnel boring machines (TBMs). The route of the MRT Blue Line project is presented in Figure 1. The project was constructed along highly congested roads in the heart of Bangkok city. The tunnel alignment is 22 km in length, including 18 underground cut-and-cover subway stations. The tunnel lining is of twin bored single-track tunnels. Each tube has an outer diameter of 6·3 m, with an inner diameter of 5·7 m of segmental lining.

A total tunnel length of 20 km (excluding underground stations) was constructed using eight earth pressure balance (EPB) shields (six Kawasaki and two Herrenknecht machines). A comparison of the EPB shield used in the project, as listed by Suwansawat (2002), has been updated and presented in Table 1. The sequences of the EPB shield drives are presented in Table 2. As shown in Figure 1, the major North and South alignments have been divided into four subsections, namely, Sections A and B for the North alignment and Sections C and D for the South alignment.

EPB shield	1 & 2	3 & 4	5 & 6	7 & 8
Section route	A North N1 – N4 & N1 – S9 + Depot	B North N4 – N9	C South S9 – S6	D South S6 – S1
Operator	Nishimatsu	Obayashi	Kumagai Gumi	Bilfinger & Berger
Specification				
Manufacturer	Kawasaki	Kawasaki	Kawasaki	Herrenknecht
Shield diameter	6·43 m	6·43 m	6·43 m	6·46 m
Typical face pressure	50 kPa	180 kPa	200 kPa	180 kPa
Cutting wheel dia. not including copy cutter	6·43 m	6·43 m	6·43 m	6·48 m
Over-excavation gap	6·5 cm	6·5 cm	6·5 cm	9 cm
Max. copy cutter stroke	10 cm	10 cm	10 cm	N.A.
Overall length	8·35 m	8·35 m	8·33 m	6·19 m
Articulation number	1 (4·39/3·94)	1 (4·39/3·94)	1 (4·39/3·94)	1 (3·275/2·915)
Number of jacks	20 × 200 t	20 × 200 t	40 × 100 t	40 × 100 t
Total thrust force	35 630 kN	35630 kN	35630 kN	28300 kN
Cutter head drive	4 × 180 kW electric motors	4 × 180 kW electric motors	4 × 180 kW electric motors	8 hydraulic motors powered by 4 × 160 kW electric pumps
Opening ratio of cutter face	60%	60%	60%	42%
Grouting				
Type of grouting	Thixotropic cement/bentonite	Thixotropic cement/bentonite	Thixotropic cement/bentonite	Bentonite, cement + fly ash
Typical pressure	2·5 bar	2 bar	2 bar	>3 bar
Typical quantities	1·8 m^3/m	1·8 m^3/m	2·2 m^3/m	N.A.
Typical grout filling ratio	120%	120%	120%	150%
Muck removal				
Operation	Screw conveyor, belt conveyor & muck car	Screw conveyor & pumping	Screw conveyor, belt conveyor & muck car	Screw conveyor, belt conveyor & muck car
Max. screw conveyor	312 m^3/h	312 m^3/h	312 m^3/h	200 m^3/h
Max. belt conveyor	150·0 m^3/h	—	—	—
Max. pumping rate	—	150·0 m^3/h	—	—
Typical slurry additive volume	2·5 m^3/m	13·0 m^3/m	NA	11·0 m^3/m
Typical excavated soil volume	45·0 m^3/m	55·0 m^3/m	NA	51·0 m^3/m

Table 1. Comparison of EPB shields used in the Bangkok MRT Blue Line project (1 bar = 100 kPa)

EPB shield	1 & 2	3 & 4	5 & 6	7 & 8
Section route	A North N1 – N4 & N1 – S9 + Depot	B North N4 – N9	C South S9 – S6	D South S6 – S1
Operator	Nishimatsu	Obayashi	Kumagai Gumi	Bilfinger & Berger
Tunnelling start date	SB 23-Apr-99 NB 30-Apr-99	SB 16-Feb-99 NB 19-Mar-99	NB 9-Jun-99 SB 25-Jun-99	SB 24 July 99 NB late August 1999
Section length (SB & NB)	6871 m, 1290 m, 631 m	4292 m, 2819 m, 2459 m	7466 m	9888 m
TBM/station interface	Station excavation incomplete, move TBM between drives except as noted	Station excavation incomplete, move TBM between drives except as noted	Skid TBM thru completed station boxes S8, S7	Skid TBM thru completed station boxes S5, S4, S3, S2
Driving sequence Refer to Figure 1	**NB**:- N1→N4 drive thru N2, N3; N1→DEPOT; S9→N1 **SB**:- N1→N4; N1→S9	N4→N6 drive thru N5; N9→N8; N7→N6; N7→N9	S9→S6	S6→S1
Best week	199 rings from both machines	231 rings from both machines	164 rings from both machines	167 rings from one machine
Best day	41 rings	43 rings	35 rings	33 rings
Alignment	Twin Tunnels 18 m apart	Twin Tunnels 18 m apart	Twin Tunnels 12–18 m apart (<2 m in Asoke Rd)	Twin & Stacked Tunnels
Maximum cover	22 m	22 m	20 m	27 (SB), 22 (NB)
Minimum cover	15 m	8 m	13 m	8 m
Minimum horizontal curve radius	200 m	190 m	300 m	200 m
Maximum gradient	+/– 4%	+ /– 2%	+/– 2%	+/– 3%
Geological conditions	stiff clay & dense fine sand	stiff clay & dense fine sand	mostly in stiff clay layer	SB:-stiff clay & sand NB:-soft to stiff clay
Max. water level above invert	7 m	7 m	10 m	9 m
Location of highest water pressures	N1 – N2	N5 – N6	S7 – S6	S3 – S2

Table 2. Driving sequences of the EPB shields

The construction methods used for the tunnelling and the underground stations of the North and South sections had different sequences, as shown in Figure 2. The contractors for the North sections (i.e. sections A and B) were to start their tunnelling works as soon as possible, with the tunnelling through the eventual station sites to be completed before the station box excavation. In contrast, the EPB shields of the North section commenced work from the Thailand Cultural Centre Station, with a launch shaft located at the north end of the station towards Huai Khwang and Sutthisan Stations, and arrived at the Ratchadaphisek Station, which was already fully excavated and with the base slab construction completed. Then, the shield was driven from the north end of Ratchadaphisek Station to Phahon Yothin Station, and involved tunnelling through the incomplete Lad Phrao Station. An illustration of the North section construction method is presented in Figure 2(a). For the South section (i.e. sections C and D), on the other hand, the underground station boxes were excavated and constructed prior to the tunnelling. Hence, the South contractor avoided the extra length of temporary tunnel, which was approximately equal to the length of the underground station box. In section C (see Figure 2(b)), the

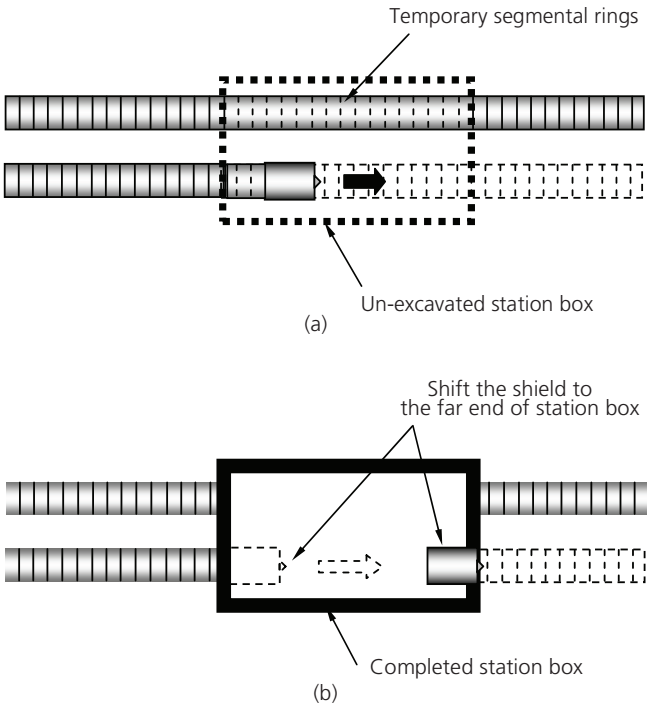

Figure 2. Construction methods for tunnelling and underground stations of the Bangkok MRT Blue Line project. (a) Construction method of the North section; (b) construction method of the South section

shield cut through the diaphragm wall at the approaching end, and then was shifted to the far end of the station box. After that, the shield was reassembled and the tunnelling recommenced. More detail on the construction methods for tunnelling and underground stations of the existing MRT Blue Line project can be found in the papers by Suwansawat (2002) and Suwansawat and Einstein (2006).

Geological condition of Bangkok subsoils

The Bangkok subsoil forms a part of the larger Chao Phraya Plain and consists of a broad basin filled with sedimentary soil deposits. These deposits form alternate layers of sand and clay. Field exploration and laboratory tests from the MRT Blue Line project show that the subsoils, down to a maximum drilling depth of approximately 60–65 m, can be roughly divided into (1) made ground at 0–1 m, (2) soft to medium stiff clays at 1–14 m, (3) stiff to very stiff clays at 14–26 m, (4) first dense sand at 26–37 m, (5) very stiff to hard clays at 37–45 m, (6) second dense sand at 45–52 m and then followed by (7) very stiff to hard clays (see Figure 3). It can be seen that the Bangkok subsoils and the layer thicknesses are homogeneous, as reported by many researchers, for example, Shibuya and Tamrakar (2003). The aquifer system beneath the city area is very complex, and the deep well pumping from the aquifers, over the last 50 years, has caused substantial piezometric drawdown in the upper soft and highly compressible clay layer as presented in Figure 3.

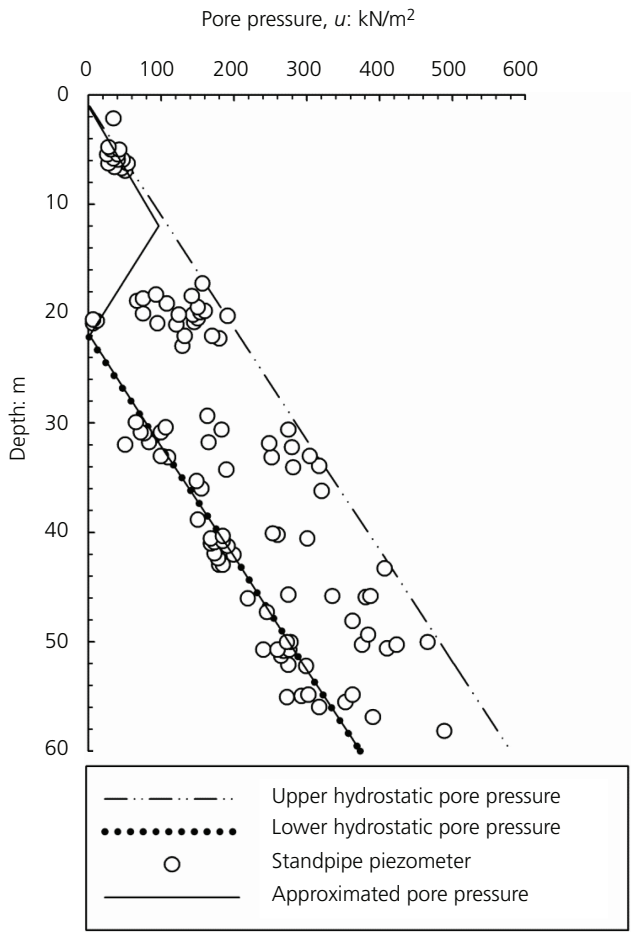

Figure 3. Pore pressure in Bangkok subsoils

Finite-element analysis for shield tunnelling

There are several methods to predict ground movements due to tunnelling. They can be categorised into three groups: empirical, analytical and numerical. The empirical methods, mostly developed from the classic work of Peck (1969), are commonly used to predict surface settlement of a single tunnel. A Gaussian curve that requires two parameters (i.e. δ_{max}, maximum settlement at tunnel centre line and i, distance of the inflection point) is employed to generate the transverse settlement trough. On the other hand, the analytical methods based on an elastic approach (Bobet, 2001; Gonzalez and Sagaseta, 2001; Lee *et al.*, 1992; Loganathan and Poulos, 1998; Rowe and Lee, 1992; Sagaseta, 1987; Verruijt and Booker, 1996) are used for the ground movement prediction during the tunnelling works. Lastly, the numerical methods based on FEM have become popular since they could model the mechanisms of the soil–structure interaction as well as accommodate realistic soil behaviour (Potts, 2003). A series of numerical studies on building response to tunnelling for London underground construction projects have been carried out by two research groups at Imperial College (Addenbrooke *et al.*, 1997; Addenbrooke and Potts, 2001; Potts, 2003) and at Cambridge University (Burland *et al.*, 2001; Mair, 2008; Wongsaroj *et al.*, 2006).

The studies have focused mainly on using in-house development of FEM codes with advanced constitutive models for predicting the tunnelling-induced ground movements.

The construction sequences for the FEM analysis of tunnelling using TBM can be divided into four major stages: (1) shield advancement and balancing pressure at the face, (2) installation of segmental lining and backfill grouting, (3) grout hardening and (4) hardened grout (Ding *et al.*, 2004; Komiya *et al.*, 1999). While tunnel excavation should be considered ideally as a 3D problem, full 3D numerical analysis is time consuming and requires excessive computational resources. Consequently, simplified 2D analysis could be considered to be sufficiently flexible and economic to find application in practice. Three simplified 2D FEMs named contraction, stress reduction and modified ground methods are employed in this study. Ground responses of the tunnel construction simulation from the three simplified 2D methods are compared in the present study. It is noted that the analyses were carried out based on short-term and uncoupled analysis assumptions.

Dimensions of finite-element model

In undertaking the 2D finite-element modelling, a sufficient mesh dimension is required. This process avoids the influence of the finite-element modelling at the boundary of the mesh model. The mesh dimensions adopted in this study follow suggestions of Möller (2006), where the maximum primary stress rotation is limited to less than 2·5° at the bottom boundary. At the left and right boundaries, the maximum vertical strain is kept to a value lower than 1% of the maximum vertical strain at the centreline. The results of his finite-element study with the HSM showed that the distance from the tunnel crown to the bottom boundary (h) should be at least 2·2 times the tunnel diameter. This criterion is restricted to cases where the tunnel diameter ranged from 4 to 12 m. The width of the finite-element model is suggested as

$$w = 2D\left(1+\frac{H}{D}\right) \quad (1)$$

where w is the width of the model, H is the distance from the ground surface to tunnel crown and D is the tunnel diameter.

Tunnelling process modelling in 2D finite-element analysis

The tunnel excavation techniques involve 3D phenomena. Simulating tunnel excavation in the 2D plane-strain finite-element analysis requires a number of assumptions to govern the missing dimension. Three simplified methods of the 2D finite-element analysis are identified as follows.

Contraction method

Vermeer and Brinkgreve (1993) proposed a 2D plain strain FEM, namely the contraction method, for ground movement computation owing to tunnelling. This method involves two calculation steps (see Figure 4). The first calculation step starts by deactivating the soil cluster within the tunnel periphery. The tunnel lining is also activated.

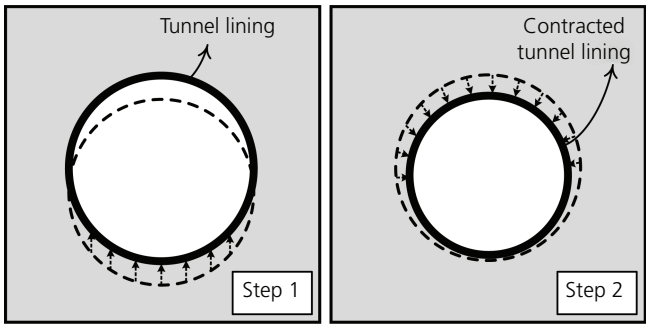

Figure 4. Calculation steps in contraction method

The tunnel lining is allowed to move upward because of the removal of the excavated soils. In the second calculation step, the tunnel lining is stepwise uniformly contracted until the pre-assigned contraction ratio is reached. This contraction ratio can be explained as

$$\text{contraction} = \frac{(\text{original tunnel area} - \text{tunnel area at current step})}{\text{original tunnel area}} \quad (2)$$

Stress reduction method

The stress reduction method, also known as the convergence-confinement method (β or λ – method), was introduced by Panet and Guenot (1982). The method uses an 'unloading factor (β)' to take into account the 3D tunnelling effects in the 2D plain strain analysis. Figure 5 shows the calculation phases of this method. The stress reduction method comprises three calculation phases. In the first calculation phase, the initial support pressure (p_o) acts on the tunnel periphery (equilibrium stage). This p_o reduces to p_β ($p_\beta = \beta p_o$; $0 < \beta < 1$) in the second calculation phase to allow the surrounding soil to deform. In the final phase, the soil cluster inside the tunnel periphery is deactivated, while the tunnel lining is activated.

Modified grout pressure method

The original grout pressure method (Möller, 2006; Möller and Vermeer, 2008) utilises the 'Gap' element to simulate the physical gap (G_p) (i.e. the gap created as a result of the larger diameter of the shield compared with the tunnel lining), as well as the grout pressure. This gap element is an interface element with the actual thickness of the physical gap. Figure 6 illustrates the finite-element installation procedure of the grout pressure method. This method is modelled by a radial pressure, which hydrostatically increases with the depth, according to a prescribed grout unit weight. One advantage of the grout pressure method is that the heaving type of ground movement profile can also be predicted, if the applied grout pressure is higher relative to the total overburden pressure above the tunnel crown.

In this study, the grout pressure method was modified. This modified method used three calculation phases (see Figure 7). In the first phase, the soil cluster inside the TBM was deactivated. Simultaneously, the face pressure was applied to an entire area of the TBM cross-section. This pressure represents the slurry pressure

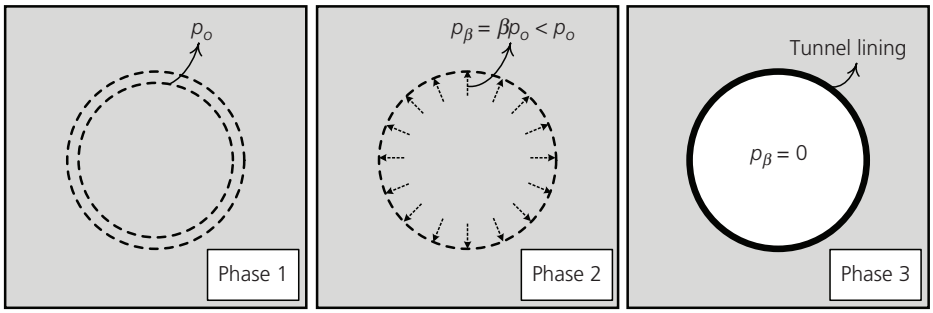

Figure 5. Calculation phases in stress reduction method

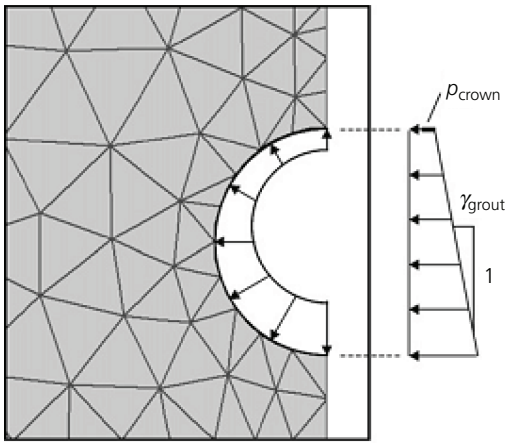

Figure 6. Finite-element procedure for shield tunnelling: grout pressure method (Möller and Vermeer, 2008)

inside the TBM chamber, which increases linearly with depth at a gradient equal to the unit weight of the slurry (γ_s). The tunnel lining, as modelled by the plate element, was activated in the second calculation phase. The area surrounding the tunnel lining representing the physical gap was then filled with fresh grout, and the grout pressure was applied to the physical gap area. The grout pressure was selected in accordance with the applied grout pressure at the tail of the TBM. The unit weight of grout (γ_g) can be used as a gradient of the grout pressure along the depth. Importantly, the continuum element was used to model the grout material. Furthermore, the cluster inside the tunnel lining was set as a dry cluster. In the last phase, the grout pressure was removed, with the physical gap area being replaced by the hardened grout material.

The advantages of separating the face pressure and the grout pressure into a two-phase calculation are as follows: (1) the face loss component can be controlled separately by the applied face pressure, and (2) the tail loss can be restricted by the actual physical

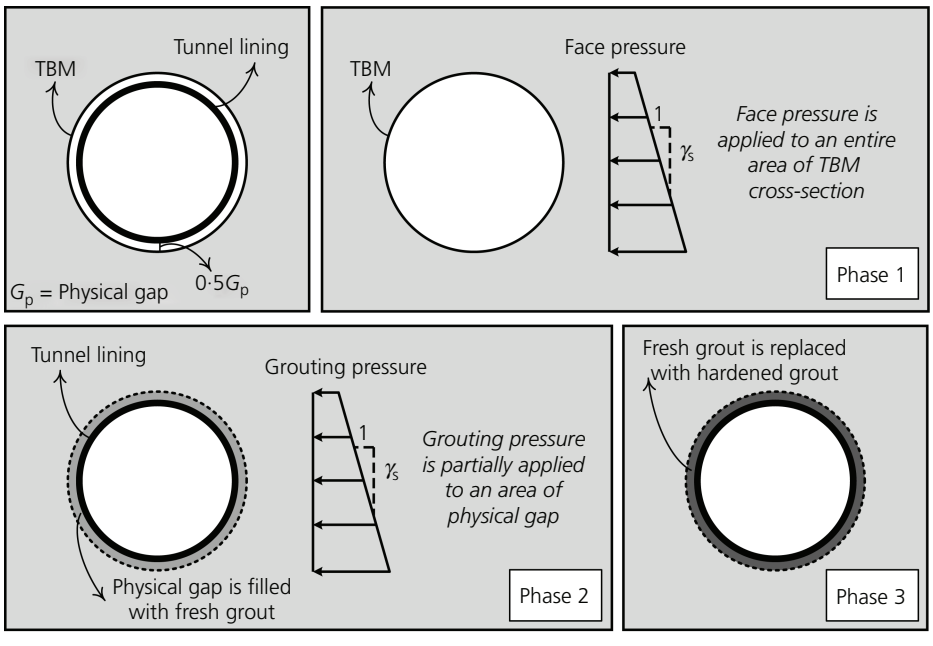

Figure 7. Calculation phases in modified grout pressure method

gap. The benefit of being able to predict the heaving type of soil movement profile, similar to the grout pressure method, is retained. Moreover, the area of the physical gap can be either contracted or expanded, depending on the applied grout pressure. One limitation of this method is that the shield loss component is ignored. This shield loss component is important as it is created by the applied pitching angle of the TBM (as the TBM is normally moved in a slightly upward angle) and the overcutting of the TBM when the tunnel alignment is curved. As a result, the modified method may be restricted to a straight alignment shield tunnelling simulation.

Constitutive soil model and its parameters

The HSM was developed under the framework of the theory of plasticity. The total strains are calculated using a stress-dependent stiffness, in which the stiffness is different in loading and unloading/reloading parts. The strain hardening is assumed to be isotropic, depending on the plastic shear and volumetric strains. A non-associated flow rule is adopted for the frictional hardening, and an associated flow rule is assumed for the cap hardening. A total of 10 input parameters are required in the HSM, as tabulated in Table 3. Schanz *et al.* (1999) explained in detail the formulation and verification of the HSM.

The stiffness and strength parameters for the HSM of soft and stiff Bangkok clays were numerically studied using PLAXIS finite-element software by Surarak *et al.* (2012). The numerical study was based on a comprehensive set of experimental data on Bangkok subsoils from oedometer and triaxial tests carried out at the Asian Institute of Technology as well as the cyclic triaxial tests carried out at Chulalongkorn University. The HSM parameters determined are the Mohr-Coulomb effective stress strength parameters together with the stiffness parameters: tangent stiffness for primary oedometer loading, secant stiffness in undrained and drained triaxial tests, unloading/reloading stiffness and the power for stress level dependency of stiffness. More details can be found in the paper by Surarak *et al.* (2012).

It should be pointed out that the Bangkok subsoils and the layer thicknesses can be assumed homogeneous, as explained earlier on. It is one of the most thoroughly studied deposits for its homogeneity and uncertainties. In general, variations in soil parameters are found to be small (Shibuya and Tamrakar, 2003). In addition, the influences of soil parameter variation on the finite-element analysis of a deep excavation in Bangkok subsoils were studied previously by Likitlersuang *et al.* (2013a).

Finite-element modelling of the Bangkok MRT Blue Line project

The contraction method, the stress reduction method, and the modified grout pressure method have been selected to model the shield tunnelling of the Bangkok MRT Blue Line project. The typical geological and pore water pressure conditions of this project are summarised in Figure 3.

Parameter	Description	Parameter evaluation
ϕ'	Internal friction angle	Slope angle of failure line based on Mohr-Coulomb
c'	Cohesion	Cohesion-intercept of failure line based on Mohr-Coulomb
R_f	Failure ratio	$(\sigma_1 - \sigma_3)_f/(\sigma_1 - \sigma_3)_{ult}$
ψ	Dilatancy angle	Ratio of $d\varepsilon_v^p$ and $d\varepsilon_s^p$
E_{50}^{ref}	Reference secant stiffness from drained triaxial test	Secant modulus at 50% peak strength at reference pressure, p^{ref}
E_{oed}^{ref}	Reference tangent stiffness for oedometer primary loading	Oedometer modulus at reference pressure, p^{ref}
E_{ur}^{ref}	Reference unloading/reloading stiffness	Unloading/reloading modulus at reference pressure, p^{ref}
m	Exponential power	Slope of trend-line in $\log(\sigma_3/p^{ref})$–$\log(E_{50})$ curve
ν_{ur}	Unloading/reloading Poisson's ratio	0·2 (default setting)
K_0^{nc}	Coefficient of earth pressure at rest (NC state)	$1 - \sin\phi'$ (default setting)

Note: p^{ref} is the reference pressure (100 kN/m^2); $(\sigma_1 - \sigma_3)_f$ is the deviatoric stress at failure based on Mohr-Coulomb; $(\sigma_1 - \sigma_3)_{ult}$ is the asymptotic value of shear strength.

Table 3. HSM input parameters

Studied sections

Seven sections from four different areas, as presented in Table 4, have been selected for the case studies. They were twin tunnels with a side-by-side pattern. The selected sections were based on the attempt to cover various combinations of soil profiles and shield operation factors encountered in engineering practice. For example, the tunnel cross-section was located entirely in stiff clay, or partially stiff clay, and clayey sand. In terms of the shield operation factors, four factors (face pressure, penetration rate, grout pressure and percentage of grout filling) were the most influential in relation to shield tunnelling. If sufficiently high levels of face pressure, grout pressure and percentage grout filling are combined with a fast penetration rate, the resulting surface settlement can be limited to an order of 10–15 mm. In contrast, if one or more shield operation factors fail to reach the required magnitude, a higher magnitude of the surface settlement is expected. Soil profiles of all seven sections, as adopted in finite-element analysis, are illustrated in Figure 8. A brief summary of the shield tunnelling parameters and the subsoil conditions encountered during the project is presented below; this summary is also given in Table 5.

Section A: 23-AR-001

The twin tunnels of this section are located entirely in the stiff clay layer. A low face pressure of 40–80 kN/m^2 was applied with a high penetration rate of 30–60 mm/min, a high grout pressure of 250–300 kN/m^2, and a high percentage of grout filling of 120% for both tunnels (i.e. Northbound (NB) and Southbound (SB)). The maximum surface settlement, after both shields had passed, was about 60 mm.

Section A: 23-G3-007-019

The twin tunnels of this section are located partially in the stiff clay and partially in the clayey sand layers. A low face pressure of 40 kN/m^2 was applied to the SB tunnel, while a higher face pressure of 80 kN/m^2 was applied to the NB tunnel. In addition, a high penetration rate of 30–40 mm/min, a high grout pressure of 250–350 kN/m^2 and high percentage of grout filling of 100–150% were applied for both the NB and SB tunnels. The maximum surface settlement, after both shields had passed, was about 45 mm.

Section		Location
A	23-AR-001	Thailand Cultural
A	23-G3-007-019	Centre – Huai Khwang
B	26-AR-001	Ratchadaphisek – Lat Phrao
C	CS-8B	Phra Ram 9 – Phetchaburi
C	CS-8D	
D	SS-5T-52e-s	Queen Sirikit National
D	SS-5T-22e-o	Convention Centre – Khlong Toei

Table 4. Location of the studied sections

Section B: 26-AR-001

The twin tunnels of this section are located partially in the soft clay and partially in the stiff clay layers. A high face pressure of 130–180 kN/m^2 was applied with a low penetration rate of 3–15 mm/min, and a high percentage of grout filling of 100–120% for both the NB and SB tunnels. A low grout pressure of 100 kN/m^2 was applied to the SB tunnel, while a higher grout pressure of 170 kN/m^2 was used in the NB tunnel. The maximum surface settlement, after both shields had passed, was about 50 mm.

Section C: CS-8B

The twin tunnels of this section are located partially in stiff clay and partially in clayey sand layers. A high face pressure of 150–200 kN/m^2 was applied to both the SB and NB tunnels along with a high penetration rate of 50 mm/min, a high grout pressure of 200 kN/m^2 and a high percentage of grout filling of 140–150%. The maximum surface settlement, after both shields had passed, was about 10 mm.

Section C: CS-8D

The twin tunnels of this section are located partially in the stiff clay and partially in the clayey sand layers. A high face pressure of 150–200 kN/m^2 was applied to both the SB and NB tunnels, along with a high penetration rate of 50 mm/min, a high grout pressure of 150–200 kN/m^2 and a high percentage of grout filling of 130–140%. The maximum surface settlement, after both shields had passed, was about 12 mm.

Section D: SS-5T-52e-s

The twin tunnels of this section are located partially in the stiff clay and partially in the hard clay layers. A high face pressure of 170 kN/m^2 was applied to both the SB and NB tunnels, along with a penetration rate of 25 mm/min, a high grout pressure of 250–400 kN/m^2 and a high percentage of grout filling of 150%. The maximum surface settlement, after both shields had passed, was about 25 mm.

Section D: SS-5T-22e-o

The twin tunnels of this section are located partially in the stiff clay and partially in the dense sand layers. A high face pressure of 200–250 kN/m^2 was applied to both the SB and NB tunnels, along with a high penetration rate of 35–40 mm/min, a high grout pressure of 400 kN/m^2 and a high percentage of grout filling of 140–150%. The maximum surface settlements after both shields had passed, was about 10 mm.

Based on all the studied cases, it can be concluded that regardless of the soil conditions encountered, the ground settlement owing to shield tunnelling is largely influenced by the shield operation factors (i.e. face pressure, penetration rate, grout pressure and percentage of grout filling).

Input parameters and finite-element model

The soil constitutive model adopted herein was the HSM. The strength and stiffness parameters used in this study were calibrated against the laboratory results from drain triaxial and oedometer

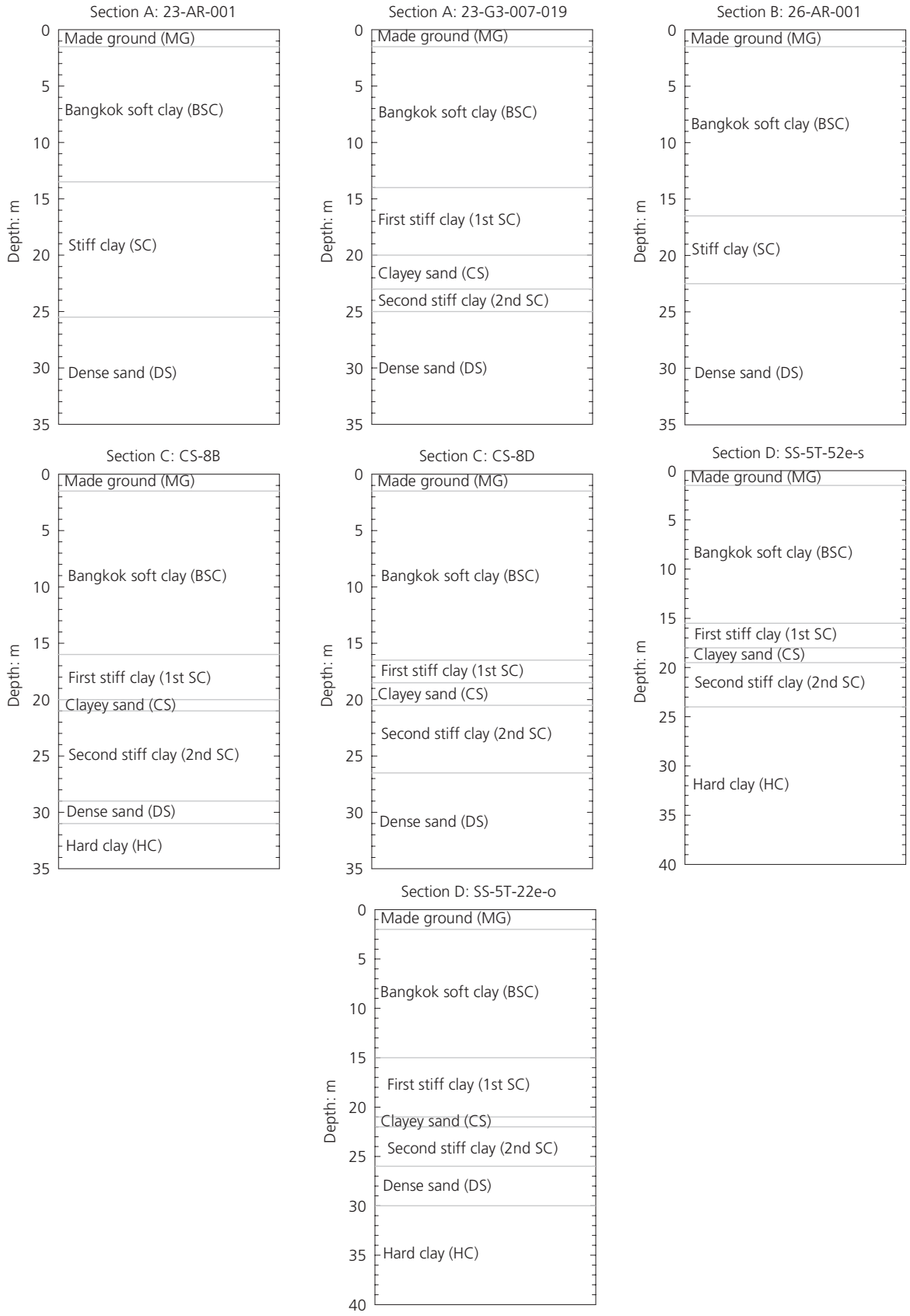

Figure 8. Soil profiles of seven sections analysed in the current study

Section		Face pressure, p_F: kN/m^2		Grout pressure: kN/m^2		Penetration rate: mm/min		Percentage of grout filling: %		Subsoils condition encountered
		SB	NB	SB	NB	SB	NB	SB	NB	Both SB and NB
A	23-AR-001	40–80	40–80	120	120	30–60	30–60	120	120	Stiff clay
A	23-G3-007-019	40	80	100–150	100–150	30–40	30–40	100–150	100–150	Stiff clay, clayey sand
B	26-AR-001	130–180	130–180	100–120	100–120	3–15	3–15	100–120	100–120	Soft clay, stiff clay
C	CS-8B	150–200	150–200	140–150	140–150	50	50	140–150	140–150	Stiff clay, clayey sand
C	CS-8D	150–200	150–200	130–140	130–140	50	50	130–140	130–140	Stiff clay, clayey sand
D	SS-5T-52e-s	170	170	150	150	25	25	150	150	Stiff clay, hard clay
D	SS-5T-22e-o	200–250	200–250	140–150	140–150	35–40	35–40	140–150	140–150	Stiff clay, dense sand

Table 5. Summary of shield tunnelling parameters and subsoil conditions

tests (Surarak *et al.*, 2012). Moreover, pressuremeter tests were used to adjust the parameters along the route of the Bangkok MRT Blue Line tunnelling (Likitlersuang *et al.*, 2013b). Table 6 presents the parameters from the HSM analysis for the MG, BSC, MC, 1st SC, CS, 2nd SC and HC layers. All soil layers are assumed to have no dilatancy ($\psi = 0°$). More detail of the parametric studies for Bangkok clays along the Bangkok MRT Blue Line can be found in the papers by Surarak *et al.* (2012) and Likitlersuang *et al.* (2013b).

The tunnel lining was modelled using the plate element with $EA = 8000$ MN/m and $EI = 56$ MNm^2/m. For the modified grout pressure method, the grout material, which fills the physical gap, was modelled by a linear elastic continuum element. The elastic modulus of the grout was assumed as 7·5 and 15 MN/m^2 for the fresh and hardened grouts, respectively. Figure 9 depicts a finite-element mesh generation of section A: 23-AR-001. The lateral movements were restricted on the left and right boundaries, and both the lateral and the vertical movements were restricted on the bottom boundary. The geometry of the model mesh generation was selected so that the conditions were satisfied. For the finite-element model shown in Figure 9, the number of elements is 3488 with an average element size of 1 m. The finer mesh size was created in the middle area, which extends at least two times the tunnel's diameter from both sides of the tunnel invert. The drawdown pore water pressure (see Figure 3) was adopted for all the studied models.

Finite-element analysis results

All seven sections of the Bangkok MRT twin tunnels were modelled using three 2D simplified methods. The details of FEM analysis and numerical results for all sections are presented in Figures 8 to 12. More details can be found in the paper by Surarak (2010).

Contraction ratio method

The contraction method was used in the first set of the analysis. The calculation steps involved the two-phase calculation, as detailed above. The values of prescribed contraction ratio were chosen so that the predicted maximum settlement matched with the measured one. The results of back-analysis using the contraction method for all seven sections are highlighted in Figures 10(a)–10(g), respectively. In general, the ground surface settlement curve, estimated from the contraction method along

Layer	Soil type[a]	γ_b: kN/m^3	c': kPa	ϕ': °	ψ: °	E_{50}^{ref}: MPa	E_{oed}^{ref}: MPa	E_{ur}^{ref}: MPa	ν_{ur}	m	K_o^{nc}	R_f	Analysis type
1	MG	18	1	25	0	45·6	45·6	136·8	0·2	1	0·58	0·9	Drained
2	BSC	16·5	1	23	0	0·8	0·85	8·0	0·2	1	0·7	0·9	Undrained
3	MC	17·5	10	25	0	1·65	1·65	5·4	0·2	1	0·6	0·9	Undrained
4	1st SC	19·5	25	26	0	8·5	9·0	30·0	0·2	1	0·5	0·9	Undrained
5	CS	19	1	27	0	38·0	38·0	115·0	0·2	0·5	0·55	0·9	Drained
6	2nd SC	20	25	26	0	8·5	9·0	30·0	0·2	1	0·5	0·9	Undrained
7	HC	20	40	24	0	30·0	30·0	120·0	0·2	1	0·5	0·9	Undrained

[a]MG, made ground; BSC, Bangkok soft clay; 1st SC, first stiff clay; CS, clayed sand; 2nd SC, second stiff clay; HC, hard clay.

Table 6. Parameters for HSM analysis

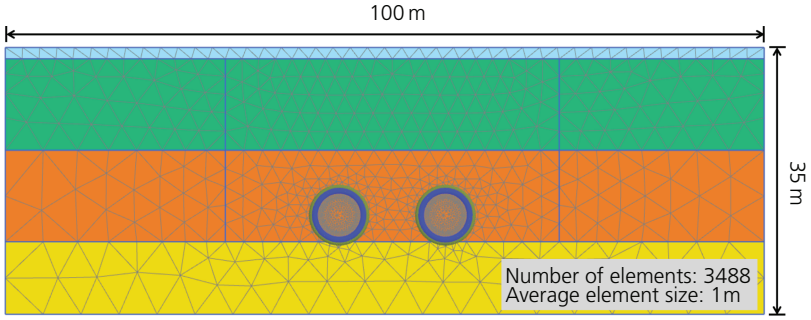

Figure 9. Typical finite-element model and mesh generation (an example from section A: 23-AR-001)

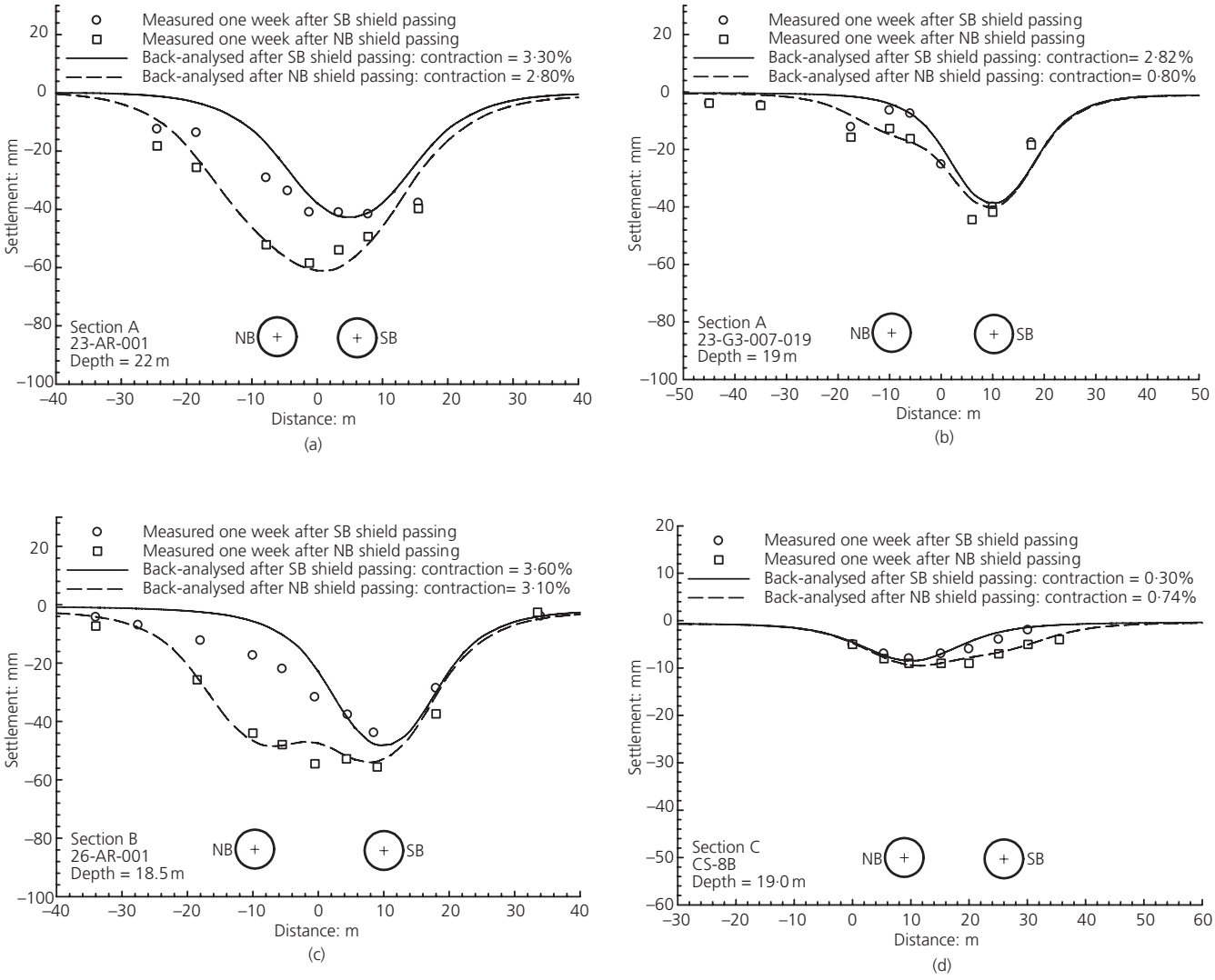

Figure 10. Results from the contraction method: (a) section A: 23-AR-001; (b) section A: 23-G3-007-019; (c) section B: 26-AR-001; (d) section C: CS-8B; (e) section C: CS-8D; (f) section D: SS-5T-52e-s; (g) section D: SS-5T-22e-o (continued on next page)

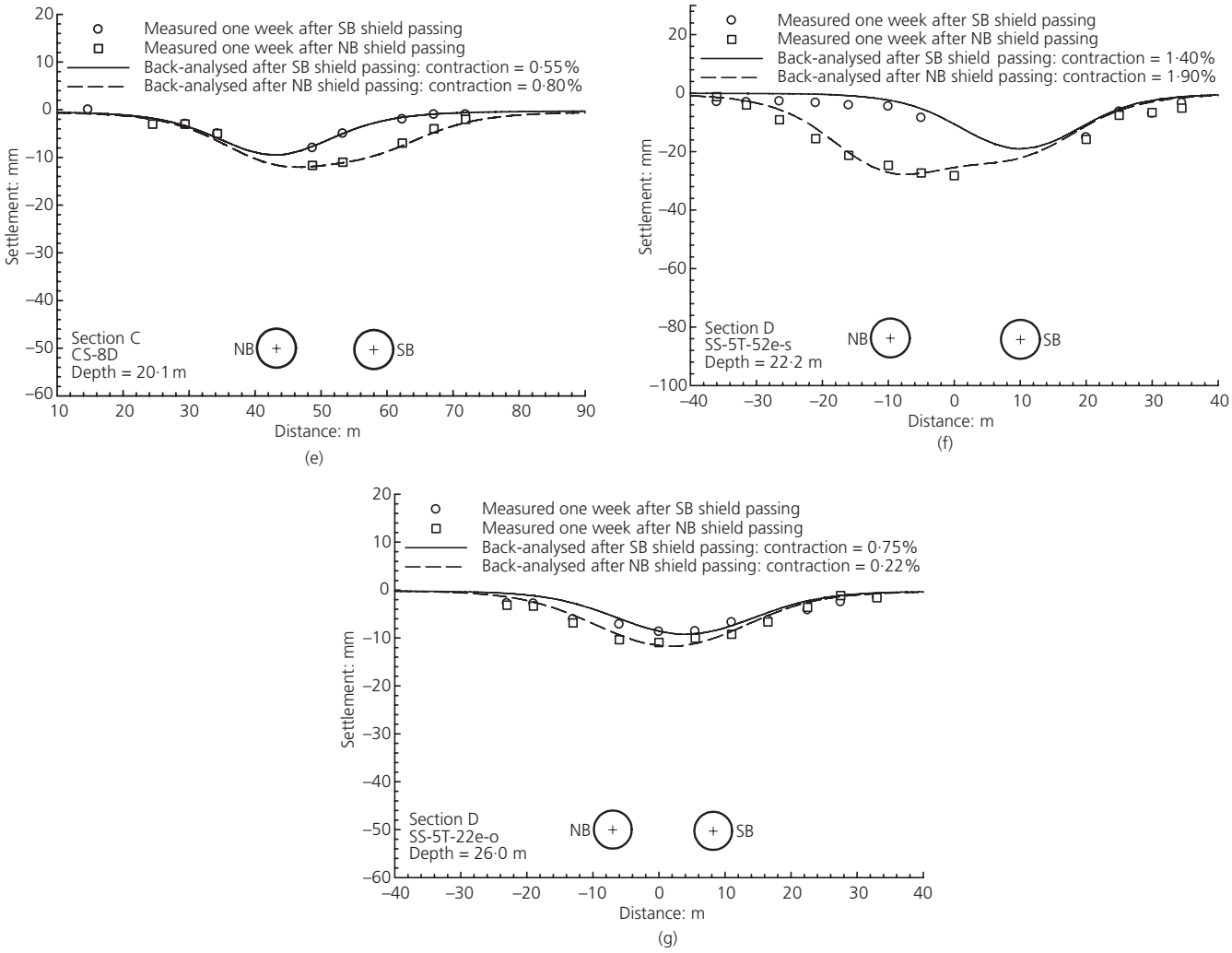

Figure 10. Continued

Section		V_L from superposition technique[a]: %		Contraction from FEM analysis: %		β value from FEM analysis	
		SB	NB	SB	NB	SB	NB
A	23-AR-001	4·86	1·67	3·30	2·80	0·40	0·45
A	23-G3-007-019	2·78	0·62	2·82	0·80	0·41	0·70
B	26-AR-001	4·41	2·67	3·60	3·10	0·53	0·62
C	CS-8B	0·27	0·74	0·30	0·74	0·84	0·72
C	CS-8D	0·43	0·69	0·55	0·82	0·76	0·71
D	SS-5T-52e-s	1·69	1·99	1·40	1·90	0·46	0·40
D	SS-5T-22e-o	0·92	0·22	0·75	0·22	0·59	0·80

[a]Superposition technique (Suwansawat and Einstein, 2006) is an improved Gaussian function based on empirical technique for twin tunnels, in which the volume loss for both tunnel excavations can be obtained.

Table 7. Volume loss from superposition technique, contraction and stress reduction factor (β) from FEM analysis

with the HSM, agrees well with the measured profiles. The back-calculated percentages of the contraction for all seven sections are listed in Table 7. The percentage of the contraction required to match the measured settlement profiles range from the values of 0·22 to 3·6. As one would expect, the larger percentage of the contraction was obtained in the case of the higher maximum surface settlement.

Stress reduction method

Similar to the study of the contraction method in the previous section, a series of finite-element back-analyses was conducted with the stress reduction method. Apart from the difference in the shield tunnel installation technique (i.e. the contraction ratio and stress reduction methods), all the other conditions in the finite-element computation were kept the same, namely, the initial stress calculation, the soil constitutive model, and the parameters used, the model geometry and the mesh generation. The values of the unloading factor (β) were selected so that the computed settlements matched the field measurements. The results from the stress reduction method back-analyses of all seven sections are presented in Figures 11(a)–11(g), respectively. The back-calculated unloading factors are listed in Table 7. It is seen that the lower values of unloading factor lead to a higher prediction of surface settlements and vice versa. This higher settlement is caused by a higher degree of stress release as less support pressure is calculated from lower values of unloading factor.

Modified grout pressure method

The last method considered herein is the modified grout pressure method. It is a three-step calculation that is applied to the finite-element analyses. Similar to the contraction ratio and the stress reduction methods, it involves a series of finite-element analyses

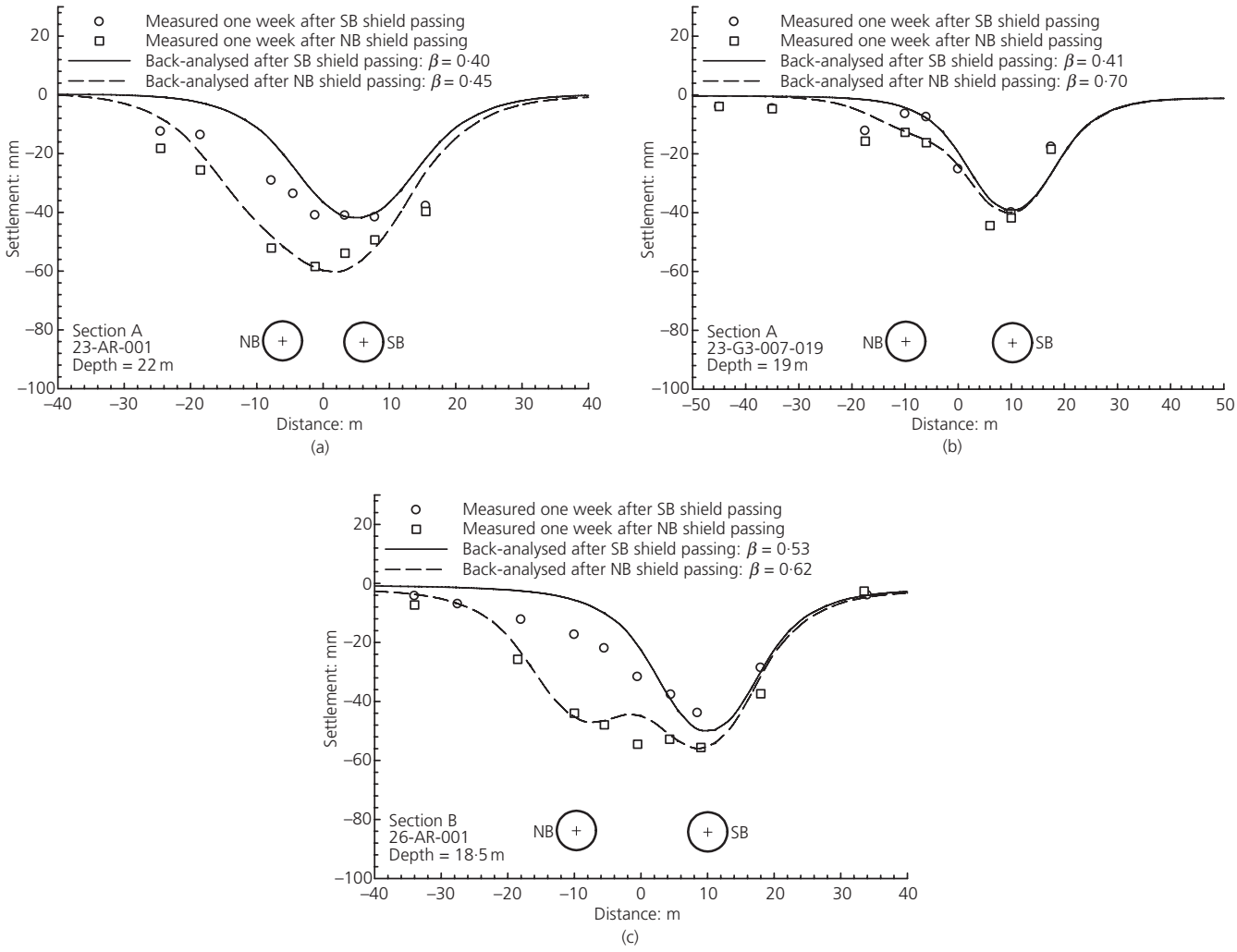

Figure 11. Results from stress reduction method: (a) section A: 23-AR-001; (b) section A: 23-G3-007-019; (c) section B: 26-AR-001; (d) section C: CS-8B; (e) section C: CS-8D; (f) section D: SS-5T-52e-s; (g) section D: SS-5T-22e-o (continued on next page)

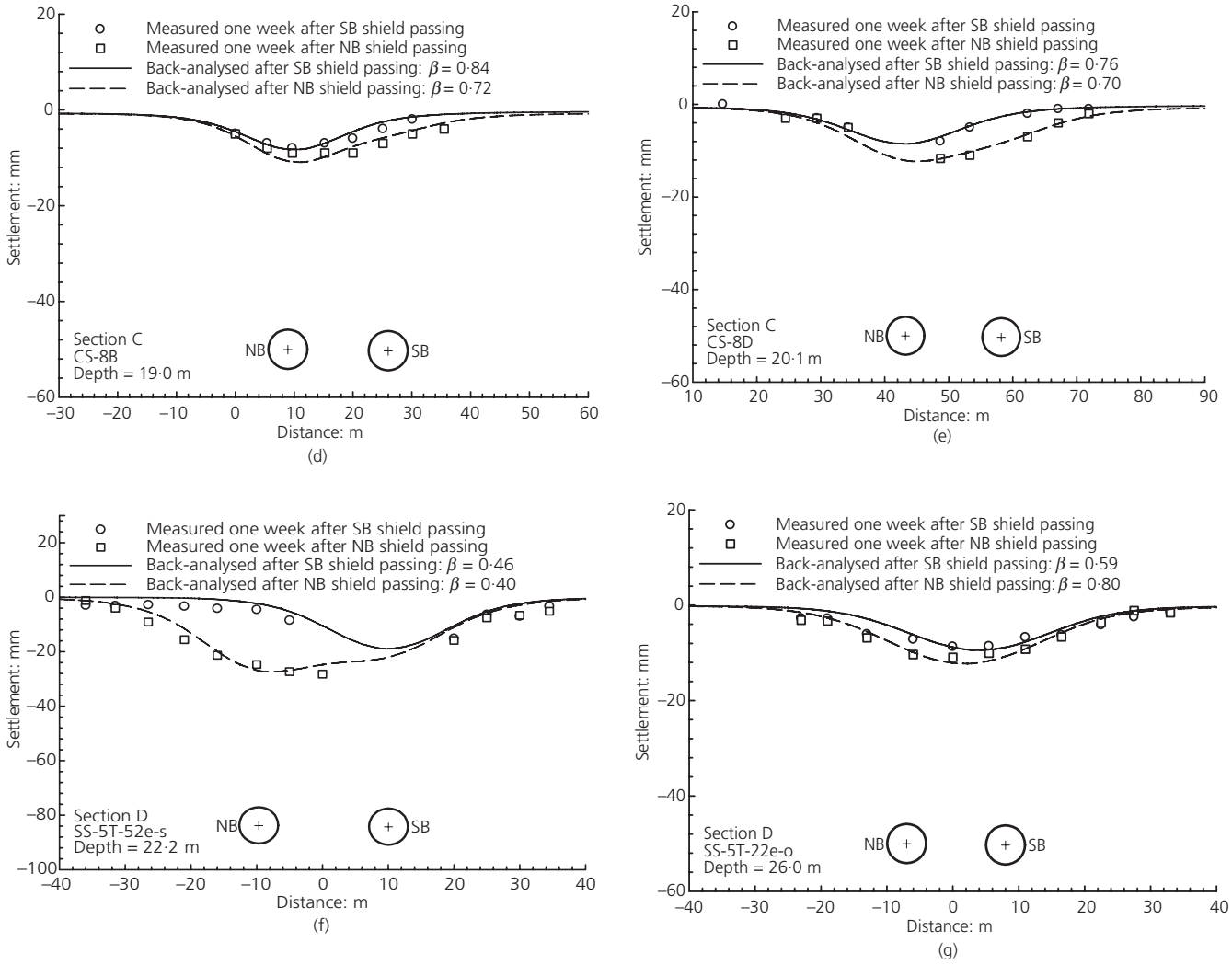

Figure 11. Continued

being undertaken for the seven twin tunnel excavation cases. In the modified grout method, the face and grout pressures were modelled by an applied pressure that increased linearly with depth. The unit weight of the slurry and grout material were assumed to be 12 and 15 kN/m^3, respectively. In the first attempt, the average face and grout pressures, as measured from the earth pressure chamber and the shield tail, were used as the face and grout pressures at the midpoint of the TBM. The average measured face and grout pressures, as used in the first attempt of the analysis, are listed in Table 8. These face and grout pressures were averaged from highly fluctuating data. As a consequence, using the measured face and grout pressures gave an over-prediction of the ground settlement, when compared with the field measurements. Furthermore, using very low face pressures of 45 and 40 kN/m^2 for the case of section A has led to an unstable (near failure) analysis. It is obvious that a higher magnitude of face pressure was needed to achieve a reasonable settlement prediction. This is perhaps understandable, because the face pressure is a measurement of the slurry pressure inside the chamber. However, a total support pressure consists of a face pressure, support from the arched soil in front of the TBM and, perhaps, a support from the TBM rotating blades.

In the second attempt, it was decided that a series of finite-element back-analyses, similar to those of the contraction method and the stress reduction methods, be performed. The results of the finite-element calculations of all seven sections are shown in Figures 12(a)–12(g), respectively, and the key results of all seven sections are listed in Table 8. In general, the predictions of the surface settlement agree well with the field measurements. The ratios of the calculated and measured face pressure were calculated for comparison. These ratios were in a wide range from 1·03 to 4·38. Nevertheless, if the low face pressure sections (section A: 23-AR-001 and 23-G3-007-019) are excluded, this range is reduced to 1·03 to 1·46, with an average value of 1·22.

Section		First tunnel excavated	Measured face pressure: kN/m²		Measured grout pressure: kN/m²		Calculated face pressure: kN/m²		Ratio of calculated/measured face pressure	
			SB	NB	SB	NB	SB	NB	SB	NB
A	23-AR-001	SB	45	70	250	152	152	175	3·38	2·50
A	23-G3-007-019	SB	40	80	300	175	175	225	4·38	2·81
B	26-AR-001	SB	140	170	100	187	187	193	1·34	1·14
C	CS-8B	NB	190	170	200	250	250	235	1·32	1·38
C	CS-8D	NB	190	200	200	245	245	230	1·29	1·15
D	SS-5T-52e-s	SB	175	170	250	185	185	175	1·06	1·03
D	SS-5T-22e-o	SB	225	250	380	240	240	365	1·07	1·46

Table 8. Measured face and grout pressures, and calculated face pressure from FEM analysis

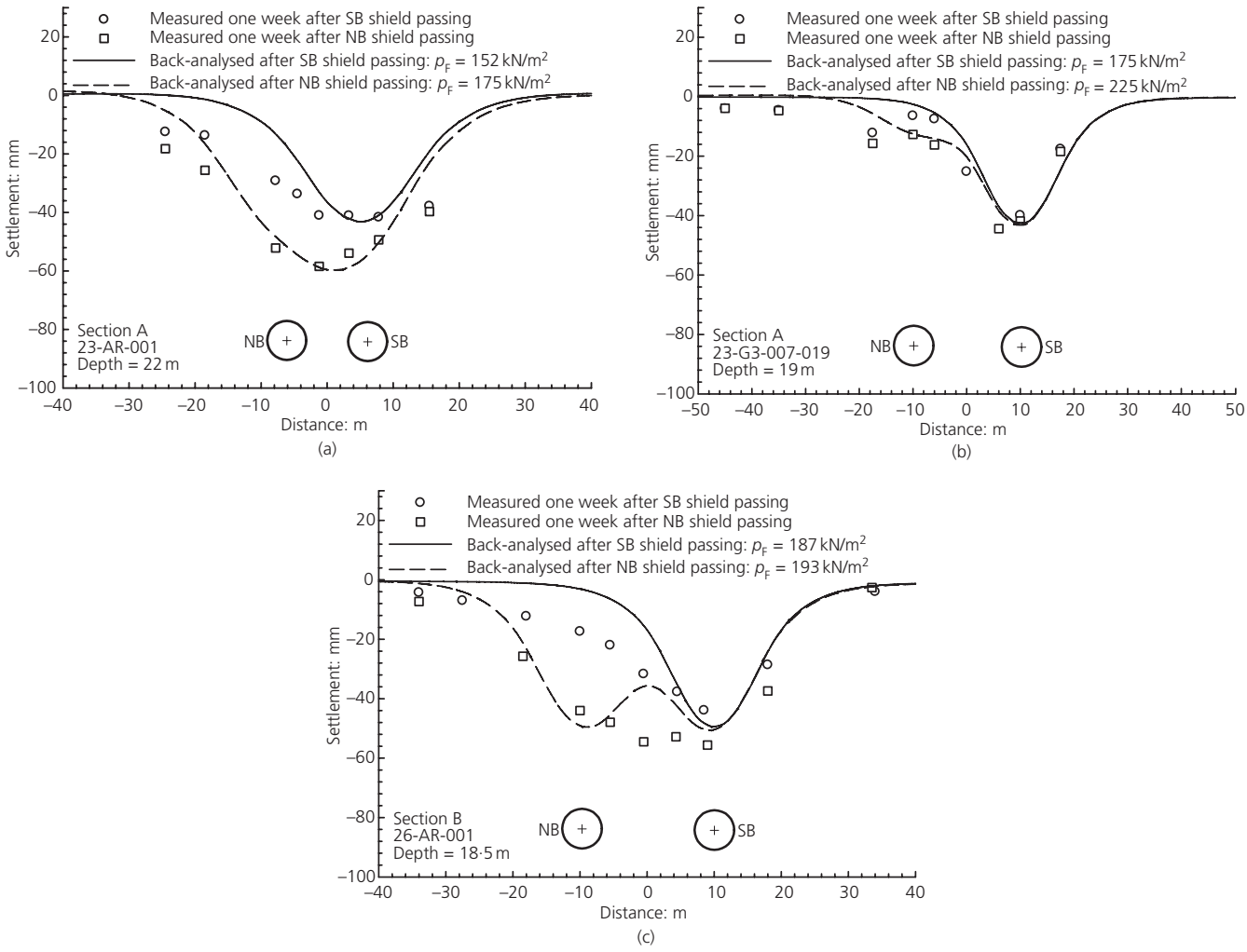

Figure 12. Results from modified grout pressure method: (a) section A: 23-AR-001; (b) section A:23-G3-007-019; (c) section B: 26-AR-001; (d) section C: CS-8B; (e) section C: CS-8D; (f) section D: SS-5T-52e-s; (g) section D: SS-5T-22e-o (continued on next page)

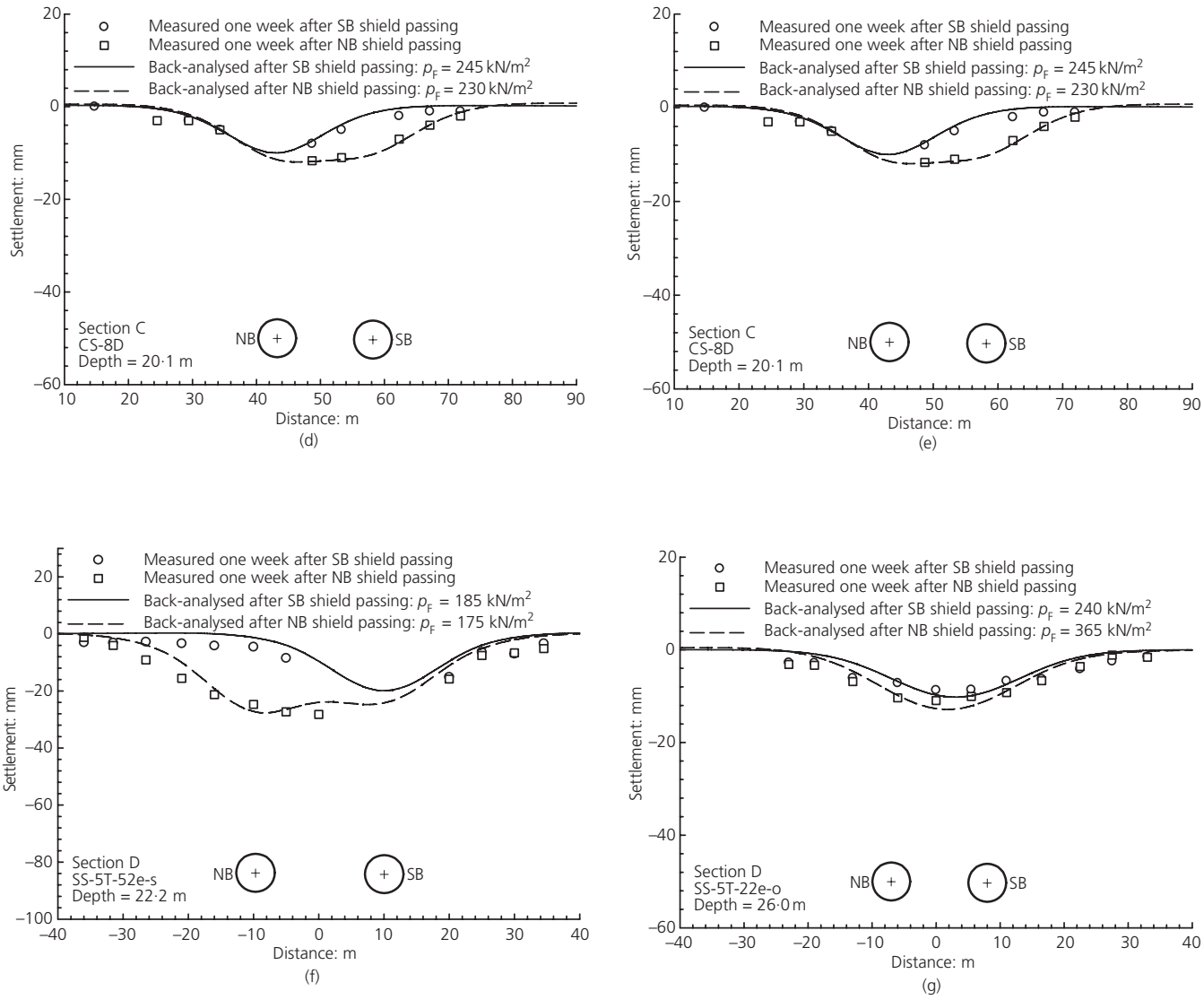

Figure 12. Continued

Relationships of contraction, stress reduction and modified grout pressure methods

In engineering practice, the ground settlement owing to the shield tunnelling is often limited by the percentage of the volume loss. One possible practical application is to establish correlations among the studied methods. In this case, the unloading factor, to be used in a finite-element analysis, can be estimated from the prescribed percentage of the volume loss (or the percentage of contraction).

The back-analysed values of the unloading factor and the percentage of the contraction are plotted in Figure 13. A fairly good correlation was obtained between the percentage of contraction and the stress reduction ratio factor, with R^2 of 0·877. However, two data points, the results from the SB and NB tunnels of section B: 26-AR-001, were excluded in the regression analysis. These volume losses for the SB and NB tunnels were high with V_L = 4·41 and 2·67%, respectively. As discussed earlier, a high face pressure of 130 to 180 kN/m^2 and the percentage of the grout filling of 120% were used in this section. As a consequence, the causes of the high volume loss, and thus the large settlement, were from the very low applied penetration rate of 3–15 mm/min and the moderately low grout pressure of 100 kN/m^2. According to Suwansawat (2002), a low penetration rate was adopted in this location as a result of the inexperienced tunnel crews who used the muck pumping technique. With this low penetration rate, the assumption of the back-analysis using the stress reduction method may not be valid. The assumption rested on the condition being undrained. However, a low penetration rate, as small as 3 mm/min, may cause the surrounding soil to be partially drained. Indeed, the back-analysed unloading factor (β) may not represent the stress release due to the tunnel excavation.

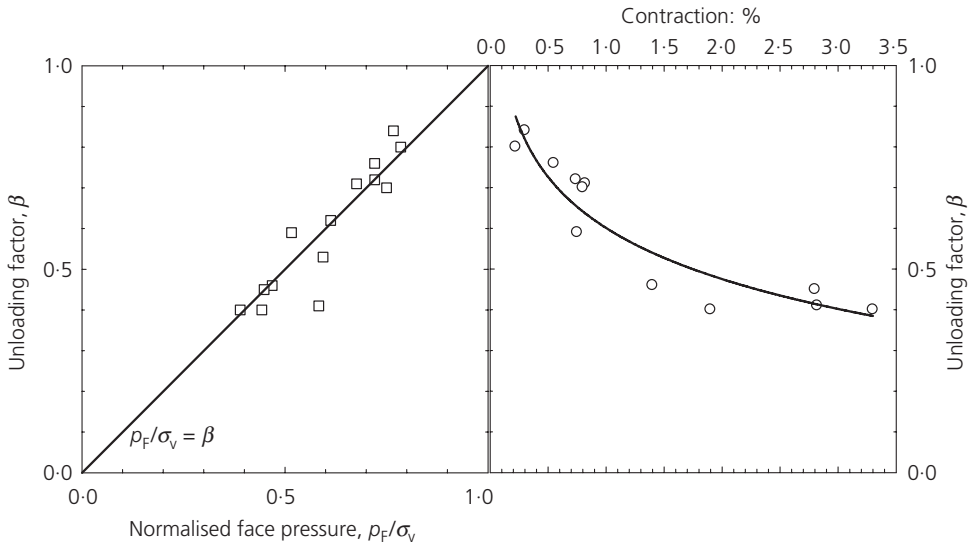

Figure 13. Relationships of contraction, stress reduction and modified grout pressure methods for all sections

The back-calculated unloading factor was plotted with the ratio of the face pressure and the total vertical stress (p_F/σ_v). As one may expect, most of the data points are located close to the $p_F/\sigma_v = \beta$ line (Figure 13). With a plot of the percentage contraction against the unloading factor on the side, correlations among the three methods can be formed. For example, if the ground settlement is limited at 1% of the volume loss, the percentage of the contraction of the tunnel lining is approximately the same in the undrained condition. From Figure 13, the unloading factor (β) reads as 0·6, which also corresponds to the face pressure (p_F) of $0{\cdot}6\sigma_v$. However, if this face pressure is applied as slurry pressure inside the TBM chamber, the surface settlement would be less than the finite-element prediction. In relation to the assumptions adopted in the finite-element analyses, Figure 13 should be employed in the cases where the TBM is operated with a high penetration rate, but with no excessive use of the copy cutter.

Concluding remarks

This study focused on the 2D finite-element analysis of the shield tunnelling. Three methods (contraction method, stress reduction method and modified grout method) were used to model tunnelling in the 2D finite-element analysis. All the clay layers (Bangkok soft clay, first and second stiff clay, and hard clay) within the selected soil profiles were modelled as undrained. This approach was taken because the resulting ground movements were compared with the field measurements immediately after construction (short term). The seven cross-sections with a side-by-side configuration were selected for this analysis. The following conclusions were drawn from the case studies.

- The calculated percentage of contraction from the finite-element analysis and the calculated percentage of the volume loss from the Gaussian curve and the superposition technique were comparable. This finding was logical as the contracted volume of the tunnel lining should be equal to the volume loss arising from the surface settlement curve in an undrained condition. A range of values from 0·22 to 4·86 and 0·22 to 3·60 were obtained for the percentage of volume loss and contraction, respectively.
- The calculated unloading factor of the studied sections ranged from 0·40 to 0·84, when the shield tunnel was operating under perfect conditions (high face pressure, high penetration rate, high grout pressure and high percentage of grout filling).
- The values of the calculated face pressure were higher than the measured one with the ratio of calculated/measured being 1·03–4·38. The higher calculated face pressure probably resulted because the actual supporting pressure consisted of the slurry pressure inside the shield chamber, the soil arching in front of the shield, and some supports from the shield element (i.e. shield blades).
- All three methods provided a sensible degree of matching for the predicted surface settlement profiles. They were also very similar in shape to the surface settlement profiles. However, all three methods have their limitations in geotechnical practice. For instance, the contraction method provides unrealistic shape of structure forces in the tunnel lining. The results cannot be used for structural lining design. The calculated pore water pressure from the stress reduction method is misread. Thus, it is not suitable for long-term analysis. In the modified grout pressure method, the shield loss component is ignored. Therefore, it should be restricted to limited tunnelling cases, as discussed earlier.
- The relationships among the three calculated parameters (percentage of contraction, unloading factor and normalised face pressure) were established. Relationships between

contraction, stress reduction and modified grout pressure methods, shown in Figure 13, can be used to approximate the values of the unloading factor or the face pressure with a given percentage of contraction or volume loss, and vice versa.

- Simplified 2D finite-element modelling can be used reasonably to solve the 3D problems of tunnelling-induced ground surface settlements. The case study from the Bangkok MRT discussed in this paper shows that 2D finite-element modelling is still very useful for solving 3D problems (e.g. tunnelling-induced settlement) in geotechnical practice. All three methods presented in this study are well known and can provide a sensible degree of matching for predicted surface settlement profiles. Practical application requires correlations among these three methods. Such correlations among the three methods are proposed in this study and can be used in geotechnical practice.

Acknowledgements

The authors wish to thank the late president of the Mass Rapid Transit Authority of Thailand (MRTA), Mr. Chukiat Phota-yanuvat, and the MRTA Engineers for their kindness in encouraging and providing relevant data for carrying out academic research activities related to such important works. The first author would like to extend his appreciation for the research funding from the Stimulus Package 2 (SP2) of the Ministry of Education, Thailand, under the theme of Green Engineering for Green Society.

REFERENCES

Addenbrooke TI and Potts DM (2001) Twin tunnel interaction – surface and subsurface effects. *International Journal of Geomechanics* **1(2)**: 249–271.

Addenbrooke TI, Potts DM and Puzrin AM (1997) The influence of pre-failure soil stiffness on the numerical analysis of tunnel construction. *Géotechnique* **47(3)**: 693–712.

Bobet A (2001) Analytical solutions for shallow tunnels in saturated ground. *Journal of Engineering Mechanics* **127**: 1258–1266.

Burland JB, Standing JR and Jardine RM (2001) *Building Response to Tunnelling – Case Studies from Construction of the Jubilee Line Extension, London*. Vol. 1: Projects and Methods. CIRIA, London, UK, CIRIA SP200.

Ding WQ, Yue ZQ, Tham LG *et al.* (2004) Analysis of shield tunnel. *International Journal for Numerical and Analytical Methods in Geomechanics* **28(1)**: 57–91.

Gonzalez C and Sagaseta C (2001) Patterns of soil deformations around tunnels: application to the extension of Madrid Metro. *Computers and Geotechnics* **28**: 445–468.

Komiya K, Soga K, Akagi H, Hagiwara T and Bolton MD (1999) Finite element modelling of excavation and advancement processes of a shield tunnelling machine. *Soils and Foundations* **39(3)**: 37–52.

Lee KM, Rowe RK and Lo KY (1992) Subsidence owing to tunnelling. I: estimating the gap parameter. *Canadian Geotechnical Journal* **29**: 929–940.

Likitlersuang S, Surarak C, Wanatowski D, Oh E and Balasubramaniam AS (2013a) Finite element analysis of a deep excavation: a case study from the Bangkok MRT. *Soils and Foundations* **53(5)**: 756–773.

Likitlersuang S, Surarak C, Wanatowski D, Oh E and Balasubramaniam AS (2013b) Geotechnical parameters from pressuremeter tests for MRT Blue Line Extension in Bangkok. *Geomechanics and Engineering: An International Journal* **5(2)**: 99–118.

Likitlersuang S, Teachavorasinskun S, Surarak C, Oh E and Balasubramaniam AS (2013c) Small strain stiffness and stiffness degradation curve of Bangkok clays. *Soils and Foundations* **53(4)**: 498–509.

Loganathan N and Poulos HG (1998) Analytical prediction for tunnelling-induced ground movements in clays. *Journal of Geotechnical and Geoenvironmental Engineering* **124**: 846–856.

Mair RJ (2008) Tunnelling and geotechnics: new horizons. *Géotechnique* **58(9)**: 695–736.

Möller SC (2006) *Tunnel Induced Settlements and Structural Forces in Linings*. Doctoral thesis, University of Stuttgart, Germany.

Möller SC and Vermeer PA (2008) On numerical simulation of tunnel installation. *Tunnelling and Underground Space Technology* **23(4)**: 461–475.

Panet M and Guenot A (1982) Analysis of convergence behind the face of tunnel. *Tunnelling'82*. The Institution of Mining and Metallurgy, London, UK, pp. 197–204.

Peck RB (1969) Deep excavations and tunnelling in soft ground. *Proceeding of the 7th International Conference on Soil Mechanics and Foundations Engineering*. State of the Art Vol., Mexico City, pp. 225–290.

Potts DM (2003) Numerical analysis: a virtual dream or practical reality? (42nd Rankine Lecture). *Géotechnique* **53(6)**: 535–573.

Rowe RK and Lee KM (1992) Subsidence owing to tunnelling. II: evaluation of a prediction technique. *Canadian Geotechnical Journal* **29**: 941–954.

Sagaseta C (1987) Analysis of undrained soil deformation due to ground loss. *Géotechnique* **37**: 301–320.

Schanz T, Vermeer PA and Bonnier PG (1999) The hardening soil model: formulation and verification. *Beyond 2000 in Computational Geotechnics* (Brinkgreve RBJ (ed.)). Taylor & Francis, Rotterdam, the Netherlands.

Shibuya S and Tamrakar SB (2003) Engineering properties of Bangkok clay. In *Proceedings of the Characterisation and Engineering Properties of Natural Soils Workshop* (Phoon KK, Hight DW, Leroueil S and Tan TS (eds)). Swets & Zeitlinger, Lisse, the Netherlands, pp. 645–692.

Surarak C (2010) *Geotechnical Aspects of the Bangkok MRT Blue Line Project*. PhD thesis, Griffith University, Australia.

Surarak C, Likitlersuang S, Wanatowski D *et al.* (2012) Stiffness and strength parameters for hardening soil model of soft and stiff Bangkok clays. *Soils and Foundations* **52(4)**: 682–697.

Suwansawat S (2002) *Earth Pressure Balance (EPB) Shield Tunnelling in Bangkok: Ground Response and Prediction*

of Surface Settlements Using Artificial Neural Networks. Doctoral thesis, Massachusetts Institute of Technology, Cambridge, MA, USA.

Suwansawat S and Einstein HH (2006) Artificial neural networks for predicting the maximum surface settlement caused by EPB shield tunnelling. *Tunnelling and Underground Space Technology* **21(2)**: 133–150.

Vermeer PA and Brinkgreve R (1993) *PLAXIS Version 5 Manual*. Balkema, Rotterdam, the Netherlands.

Verruijt A and Booker JR (1996) Surface settlements due to deformation of a tunnel in an elastic half plane. *Géotechnique* **46(4)**: 753–756.

Wongsaroj J, Soga K and Mair RJ (2006) Modelling of long-term ground response to tunnelling under St James's Park London. *Géotechnique* **57(1)**: 75–90.